



OPEN ACCESS

EDITED BY

Kaoru Tominaga,
Jichi Medical University, Japan

REVIEWED BY

Mallika Somayajulu,
Wayne State University, United States
Rogério Saad Vaz,
Federal University of Paraná, Brazil

*CORRESPONDENCE

Xiao Lin

✉ linxiao@nwpu.edu.cn

Tao Zhang

✉ zhangt@mistinechina.com

RECEIVED 07 January 2025

ACCEPTED 26 February 2025

PUBLISHED 28 March 2025

CITATION

Xu Y, Liu Y, Li J, Li Y, Xu L, Dong K, Lin X and
Zhang T (2025) Unveiling a novel *in-vitro*
model of skin inflammaging.
Front. Med. 12:1556680.
doi: 10.3389/fmed.2025.1556680

COPYRIGHT

© 2025 Xu, Liu, Li, Li, Xu, Dong, Lin and
Zhang. This is an open-access article
distributed under the terms of the [Creative
Commons Attribution License \(CC BY\)](#). The
use, distribution or reproduction in other
forums is permitted, provided the original
author(s) and the copyright owner(s) are
credited and that the original publication in
this journal is cited, in accordance with
accepted academic practice. No use,
distribution or reproduction is permitted
which does not comply with these terms.

Unveiling a novel *in-vitro* model of skin inflammaging

Ying Xu¹, Yue Liu¹, Junxiang Li², Yao Li², Linlin Xu³, Kun Dong³,
Xiao Lin^{4*} and Tao Zhang^{1*}

¹Better Way (Shanghai) Cosmetics Co. Ltd., Shanghai, China, ²AGECODE R&D Center, Yangtze Delta Region Institute of Tsinghua University, Jiaxing, Zhejiang, China, ³School of Light Industry Science and Engineering, Beijing Technology and Business University, Beijing, China, ⁴Key Laboratory for Space Biosciences and Biotechnology, School of Life Sciences, Northwestern Polytechnical University, Xi'an, China

Introduction: Sensitive skin is characterized by a disrupted skin barrier, making it prone to reacting to external stimuli, including UV exposure, air pollution, and cosmetic allergens. Sensitive skin tends to react with oxidative stress factors that could further lead to inflammation and subsequently result in inflammaging. However, there are almost no existing inflammaging models specifically for sensitive skin, highlighting the need to develop a method for screening anti-inflammaging ingredients and products.

Methods: An *in vitro* macrophage-fibroblast model was established to evaluate the anti-inflammaging effects of the ingredients. The M1 phenotype and aging-associated gene expression were assessed using qPCR to validate the inflammaging model. RNA sequencing was used to further elucidate the inflammaging mechanisms of the two validated ingredients.

Results and conclusion: A novel *in-vitro* model of sensitive skin inflammaging was developed by applying the supernatant of the M1 macrophage culture medium to induce cellular senescence in fibroblast cells, facilitating the screening of anti-inflammaging ingredients. In this model, supramolecular bakuchiol could promote collagen COL1A1 and COL3A3 production and inhibit inflammatory factors by enhancing the transcription of anti-inflammatory genes (*PTX3*, *ADAM33*, and *PDLIM1*), while *Terminalia chebula* extract inhibits cell senescence by reducing the transcription of *MAP4K2* and the accumulation of the inflammatory factor *CCL3*.

KEYWORDS

sensitive skin, inflammaging, bakuchiol, *Terminalia chebula* extract, RNA-seq

1 Introduction

The skin is the largest organ in the human body. As people age, senescent skin cells gradually accumulate and can produce the senescence-associated secretory phenotype (SASP) to affect adjacent cells, resulting in the reduction of skin thickness, regenerative capacity, and barrier effect (1–3). López-Otín et al. proposed 12 hallmarks of aging in 2023 (4). Chronic inflammation, one of the hallmarks of aging, is accompanied by systemic manifestations as well as local pathological phenotypes (5).

Inflammaging skin is a kind of skin aging phenotype resulting from sterile, low-grade chronic inflammation. As aging progresses, inflammation intensifies, generating numerous molecules such as ROS, IL-1, IL-6, IL-8, TNF- α , and MMPs (6, 7), exacerbating skin oxidation and glycation, releasing more free radicals and inflammatory factors while degrading collagen and elastin, thereby accelerating the signs of cellular and skin aging, including wrinkles, sagging, pigmentation, and dullness (8–10).

Sensitive skin, also known as fragile skin or reactive skin, is characterized by a disrupted skin barrier that is often prone to reactions from external stimuli, including UV exposure, air pollution, and cosmetic allergens (11). According to a global questionnaire study, 77.3% of panelists, regardless of gender, reported having sensitive facial skin (12). Compared to normal skin, sensitive skin often experiences chronic inflammation for extended periods, making it more susceptible to inflammaging (13, 14). For those with sensitive skin, anti-inflammaging is a crucial way to prevent skin aging. On one hand, there are only a limited number of *in vitro* models for sensitive skin; the main research studies focus on animal models or clinical studies, which tend to be complex and are not conducive to the rapid screening of cosmetic ingredients (14, 15). On the other hand, there are nearly no models for studying inflammaging in sensitive skin, indicating the need to develop methods for screening anti-inflammaging ingredients and products.

There are several anti-aging ingredients used in cosmetic products for sensitive skin, such as bakuchiol, which is sourced from *Psoralea corylifolia* Linn (16, 17). Bakuchiol enhances collagen renewal and refines skin tone and texture, potentially serving as a safer alternative to retinol (18). Supramolecular bakuchiol is composed of bakuchiol, matrine, and vitamin E through non-covalent bonds. Matrine has been proven to possess effective anti-inflammatory properties by significantly inhibiting the production of inflammatory factors such as TNF- α (19). However, further investigation is required to determine whether supramolecular bakuchiol could be applied as a potential agent for anti-skin inflammaging. *Terminalia chebula* extract is another ingredient that has demonstrated notable anti-oxidative, anti-inflammatory, and anti-aging effects (20). Similar to supramolecular bakuchiol, there are limited studies focusing on whether *Terminalia chebula* extract could serve as a potential agent for anti-skin inflammaging due to the lack of an appropriate model.

Horiba et al. showed that M1 macrophages could induce cellular senescence in fibroblast cells (21). Based on this study, we developed a novel *in vitro* model of skin inflammaging by using an M1 macrophage supernatant to induce HSF cell aging. Using this model, we confirmed the anti-inflammaging effects of *Terminalia chebula* extract and supramolecular bakuchiol and aimed to explain the regulatory mechanisms using mRNA-sequence techniques.

2 Materials and methods

2.1 Experiment materials

The THP-1 cell lines used in this study were obtained from Wuhan Pricella Biotechnology Co., Ltd., while the HSF cell lines were sourced from Newgainbio. *Terminalia chebula* extract (Yingge), matrine, lauric acid (Sigma Aldrich), bakuchiol (Shanghai

Youtian Industrial Co., Ltd.), hydroxypinacolone retinoate (Grant Chemical Company), cell culture medium (WISENT, high glucose; Servicebio, RPMI1640 medium), high-quality fetal bovine serum (Gibco), phosphate buffered saline (Basal Media, PBS), trypsin (Basal Media, Trypsin, 0.25%), Cell Counting Kit-8 (Dojindo, CCK-8), cell culture flasks (Thermo, T75), cell culture plates (Corning, 96-well, 6-well, and 12-well), pipettes (Thermo, 5 mL and 15 mL), centrifuge tubes (Corning, 15 mL), a disposable cell counting plate (Countstar), a qPCR octuple with an optical flat cap (Abclonal), lipopolysaccharide (Beyotime, LPS), phorbol ester (Beyotime, PMA), interferon- γ (Yufeng Biology, IFN- γ), transforming growth factor β 1 (Novoprotein, TGF- β 1), RNA extraction kit (Omega), RNA reverse transcription kit (Beyotime), and a 2 \times Universal SYBR Green Fast qPCR mix (Abclonal) were all utilized in the study.

2.2 Experiment equipment

The experiment utilized a variety of equipment, including an adjustable pipette (Eppendorf), an analytical balance (Sartorius), an inverted microscope (Motic), a low-speed centrifuge (HealForce), a refrigerated centrifuge (available instrument), a nucleic acid quantitative instrument (Thermo Fisher), a PCR instrument (Takara), a real-time fluorescence quantitative PCR instrument (Thermo Fisher), a constant temperature incubator (HealForce), an electric pipette (Eppendorf), a cell counter (Countstar), an ultraclean bench (Thermo), a digital display constant temperature water bath (Lanbao Haibo Biology), a liquid nitrogen tank, a refrigerator (Haier), and a multifunctional microplate reader (PerkinElmer).

2.3 Experimental methods

2.3.1 Preparation of supramolecular bakuchiol

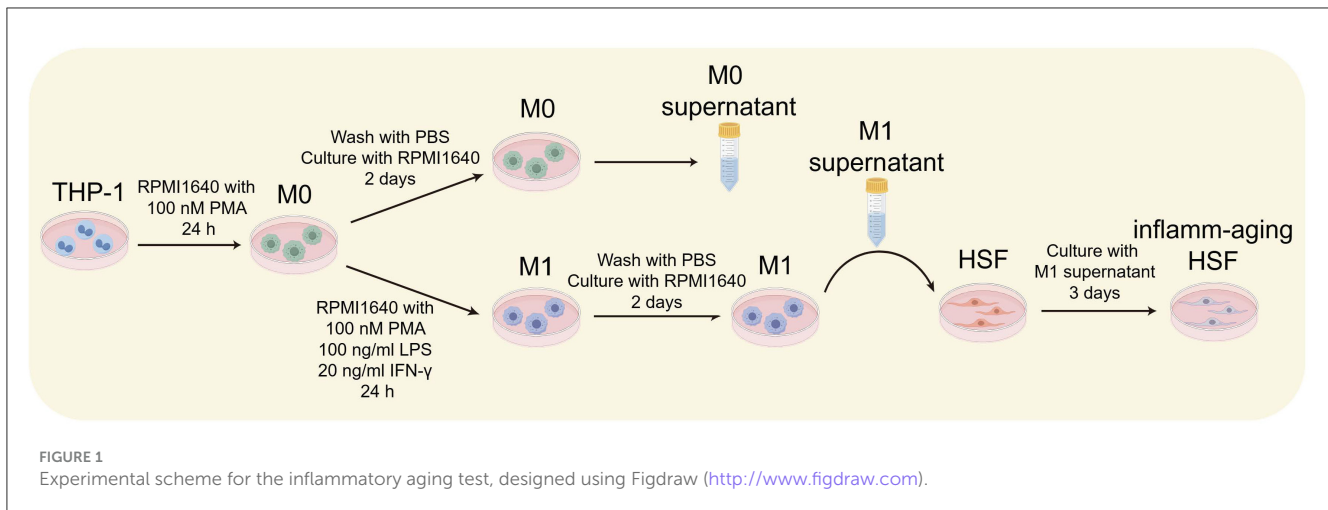
Supramolecular bakuchiol was prepared as previously described (22), involving two steps.

Preparation of Mat-LA IL: A specific amount of matrine and lauric acid was dissolved in ethanol and stirred at 30°C for 4 h. The molar ratio of matrine to lauric acid was 1:1. After the reaction was complete, the solvent was removed by vacuum distillation at 60°C, and the resulting matrine lauric acid IL was stored in a vacuum dryer containing phosphorus pentoxide, and it was named Mat-LA IL.

Preparation of supramolecular bakuchiol: A specific quantity of the prepared Mat-LA IL was added to a solution of bakuchiol and stirred in the dark at 30°C for 24 h. The molar ratio of Mat-LA IL to bakuchiol is 1:1. After the reaction was completed, supramolecular bakuchiol was obtained by filtering through a 0.22 μ m filter membrane and stored in a light-shielded dryer.

2.3.2 Cell viability assay

The viability of cells was determined using the Cell Counting Kit-8 (Dojindo, CCK-8) according to the manufacturer's instructions (23). Cells were grown in a 96-well plate until they reached 50% to 70% confluency. In the blank control group, 100 μ L of culture medium was added to each well. Each well in



the sample group received 100 μL of culture medium containing the specified sample concentration. In contrast, the zero group was not inoculated with cells and received only 100 μL of cell culture medium. After adding the samples, the 96-well plate was cultured for 24 ± 2 h. The supernatant was then removed, and the CCK-8 working solution was added and incubated at 37°C for 2 ± 0.5 h in the dark. After incubation, the absorbance was measured at 450 nm. Cell viability was calculated using the following equation according to the manufacturer’s instructions.

$$\text{Cell viability (\%)} = \frac{\text{sample group OD} - \text{zero group OD}}{\text{blank group OD} - \text{zero group OD}} \times 100\%$$

2.3.3 In vitro model of skin inflammaging

The protocol involved inducing inflammation with M1 macrophages and inducing cellular aging in HSF cells using M1 macrophage supernatant (Figure 1) (21).

2.3.3.1 Induction and identification of M1 macrophages

Induction of M1 macrophages:

Induction of M0 macrophages: THP-1 cells were centrifuged at low speed, resuspended, and counted. A complete RPMI 1640 medium containing 100 nM PMA was prepared. The cells were inoculated in 6-well plates at a density of 1 × 10⁶ cells per well and incubated for 24 h to induce the M0 macrophages.

Induction of M1 Macrophages: RPMI 1640 complete medium containing 100 nM PMA, 100 ng/mL LPS, and 20 ng/mL IFN-γ was prepared. The culture medium of M0 macrophages was removed, and the prepared medium was added to each well. After 24 h, M0 macrophages were induced into M1 macrophages.

Identification of M1 macrophages:

M0 group: After the previous step, M0 macrophages were obtained by treating them, and PBS was used for washing. Then, 3 ml of RPMI1640 complete culture medium was added to each well to culture for 2 days, and RNA was extracted.

M1 group: After obtaining M1 macrophages through the previous step, we used PBS for washing. Then, 3 ml of RPMI1640

complete culture medium was added to each well and cultured for 2 days. The supernatant was then collected, and RNA was extracted. To determine whether the expression of CD86, TNF-α, IL-1β, and IL-6 mRNA in M1 macrophages was upregulated compared to M0 macrophages, qRT-PCR was performed. The qRT-PCR primers were 5’-GGAGCGAGATCCCTCCAAAAT-3’ (GAPDH forward) and 5’-GGCTGTTGTCATACTTCTCATGG-3’ (GAPDH reverse); 5’-CCTGCTCATCTATACACGGTTACC-3’ (CD86 forward) and 5’-CGTCGTACAGTTCTGTGACATTATC-3’ (CD86 reverse); 5’-CTCATCTACTCCCAGGTCCTCTTC-3’ (TNF-α forward) and 5’-CGATGCGGCTGATGGTGTG-3’ (TNF-α reverse); 5’-AGGGCTCCTCGGCAAATGTA-3’ (IL-6 forward) and 5’-GAAGGAATGCCATTAACAACAA-3’ (IL-6 reverse); 5’-TGGCTTATTACAGTGGCAATGAGG-3’ (IL-1β forward) and 5’-AGTGGTGGTCGGAGATTCGTAG-3’ (IL-1β reverse). qRT-PCR assays were conducted under the following cycling conditions: 95°C for 3 min, followed by 40 cycles of 95°C for 5 s and 60°C for 30 s.

2.3.3.2 Induction of inflammaging on HSF cells

HSF cells were seeded in a 12-well plate, achieving a final cell density of 1 × 10⁴ cells per well. The cells were then cultured for 24 h. Various groups were added as indicated and maintained for 3 days. After this period, RNA was extracted, and the expression levels of *p16*, *p21*, *COL1A1*, and *MMP-1* genes were detected using qRT-PCR. The qRT-PCR primers used were 5’-GGAGCGAGATCCCTCCAAAAT-3’ (GAPDH forward) and 5’-GGCTGTTGTCATACTTCTCATGG-3’ (GAPDH reverse); 5’-GCCCAACGCACCGAATAGTTAC-3’ (p16 forward) and 5’-GCAGCAGCTCCGCCACTC-3’ (p16 reverse); 5’-CCCGTGAGCGATGGAAGTTC-3’ (p21 forward) and 5’-GCCTGCCTCCTCCCAACTC-3’ (p21 reverse); 5’-CCTGGAAAGAATGGAGATGA-3’ (COL1A1 forward) and 5’-ACCATCCAAACCACTGAAAC-3’ (COL1A1 reverse); 5’-ATGAAGCAGCCCAGATGTGGAG-3’ (MMP-1 forward) and 5’-TGGTCCACATCTGCTCTTGGCA-3’ (MMP-1 reverse). qRT-PCR assays were performed under the following cycling conditions: 95°C for 3 min followed by 40 cycles of 95°C for 5 s and 60°C for 30 s.

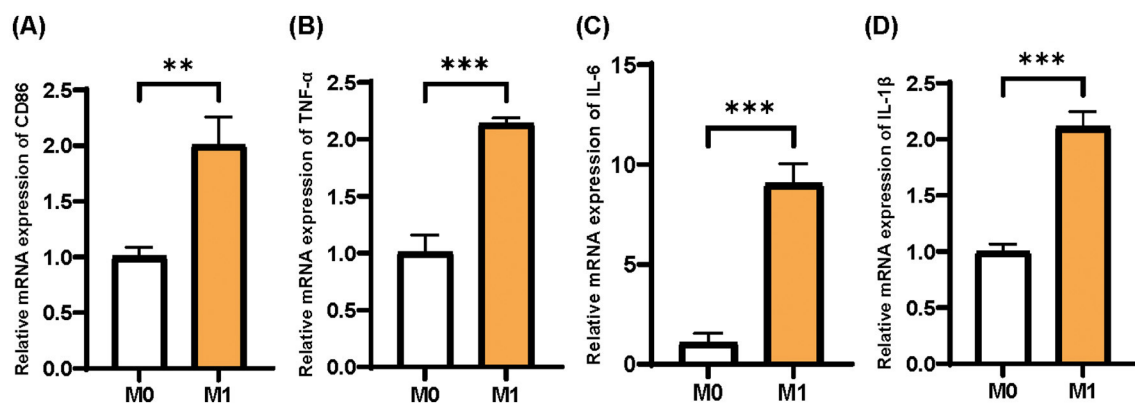


FIGURE 2 Identification of M0 and M1 phenotypes of THP-1 cells. (A) CD86; (B) TNF- α ; (C) IL-6; (D) IL-1 β . Mean \pm SD, $n = 3$.

2.3.4 RNAseq test for supramolecular bakuchiol and Terminalia chebula extract

Total RNA was extracted using Trizol reagent (Invitrogen, CA, USA) following the manufacturer's protocol. RNA sequencing was conducted by Lianchuan Biotechnology Co., Ltd. (China). Cutadapt software (<https://cutadapt.readthedocs.io/en/stable/>, version: cutadapt-1.9) was used to eliminate reads that contained adapter contamination (command line: `~cutadapt -a ADAPT1 -A ADAPT2 -o out1.fastq -p out2.fastq in1.fastq in2.fastq -O 5 -m 100`).

After removing the low-quality bases and undetermined bases, we used HISAT2 software (<https://daehwankimlab.github.io/hisat2/>, version: hisat2-2.0.4) to map reads to the genome. The mapped reads for each sample were assembled using StringTie (<http://ccb.jhu.edu/software/stringtie/>, version: stringtie-1.3.4d.Linux_x86_64) with default parameters (command line: `~stringtie -p 4 -G genome.gtf -o output.gtf -l sample.input.bam`). Then, all transcriptomes from every sample were merged to reconstruct a comprehensive transcriptome using gffcompare software (<http://ccb.jhu.edu/software/stringtie/gffcompare.shtml>, version: gffcompare-0.9.8.Linux_x86_64). After generating the final transcriptome, StringTie and ballgown (<http://www.bioconductor.org/packages/release/bioc/html/ballgown.html>) were used to estimate the expression levels of all transcripts and calculate the expression level for mRNAs by determining FPKM ($FPKM = \frac{\text{total_exon_fragments}}{\text{mapped_reads}(\text{millions})} \times \text{exon_length}(\text{kB})$), (command line: `~stringtie -e -B -p 4 -G merged.gtf -o samples.gtf samples.bam`).

We then compared the RNA expression levels (FPKM values) across different sample groups using DESeq2 software. Expressed RNA was identified with P values < 0.05 and $|\text{fold change}| > 1.5$. RNA with fold changes > 1.5 was labeled as upregulated genes (up), while those with fold changes < -1.5 were labeled as downregulated genes (down). Differentially expressed RNAs were visualized using a volcano plot, and the selected differentially expressed RNAs were analyzed with a heatmap. Gene ontology (GO) (<http://www.geneontology.org>) and Kyoto Encyclopedia of Genes and Genomes (KEGG) (<http://www.genome.jp/kegg/>) analyses were conducted using bioinformatics, with $p < 0.05$

considered significant, and plotted via <https://www.bioinformatics.com.cn>, an online platform for data analysis and visualization (24).

2.4 Statistical analysis

All experiments were conducted with a minimum of three biological replicates. All experimental data were statistically analyzed using GraphPad Prism 9 software. An unpaired Student's t -test was used to assess whether there was a significant difference between the two groups. P -values < 0.05 were considered statistically significant.

3 Results

3.1 Induction and identification of M1 macrophages

According to the previous study, CD86, TNF- α , IL-1 β , and IL-6 were found to be important inflammatory markers for M1 macrophages induced by THP-1 cells (21). Based on the qPCR test, the mRNA expressions of CD86, TNF- α , IL-1 β , and IL-6 in M1 macrophages were significantly higher than those in M0 macrophages, indicating that the induction of M1 macrophages was successful (Figure 2).

3.2 Induction of inflammaging on HSF cells

We collected the culture medium of M1 macrophages and used the supernatant to culture HSF cells. After 3 d, we detected the cellular senescence indicators p16 and p21, along with skin aging-related indicators MMP-1 and Col-1, via qPCR. Compared to the blank control 1,640 group, the expression levels of p16, p21, and MMP-1 mRNA in the negative control M1 group were significantly upregulated, while the expression of Col-1 was significantly downregulated. Additionally, the positive control TGF- β 1 group significantly downregulated the expression of p16,

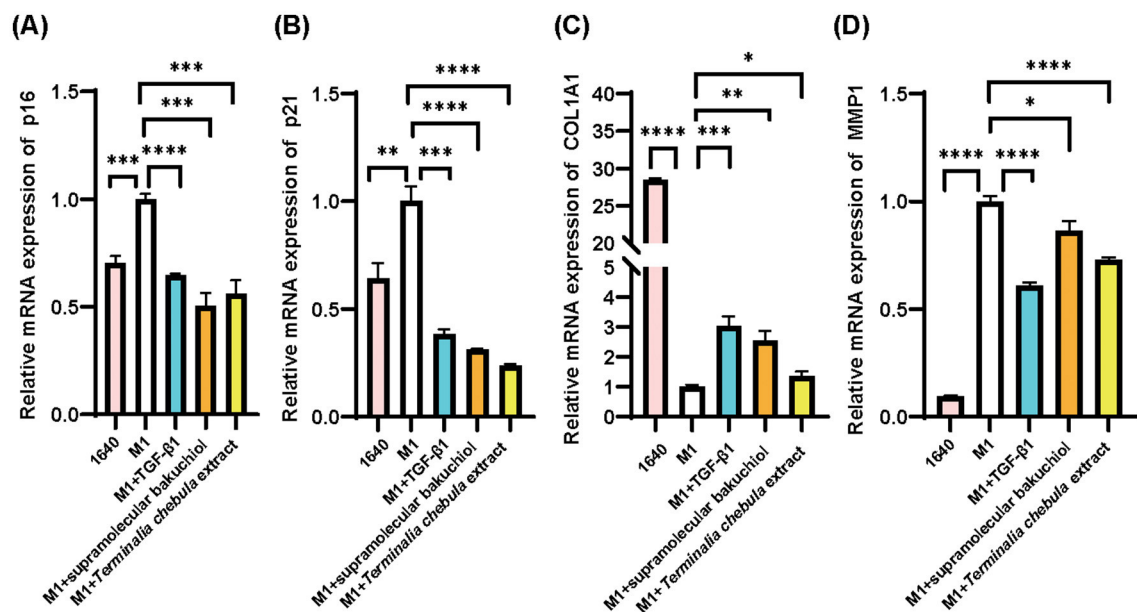


FIGURE 3 HSF cell inflammatory senescence assay for the results of the anti-inflammatory senescence test of the samples: 1640: RPMI1640 medium, M1: M1 macrophage supernatant, sample group: M1 macrophage supernatant plus each sample (TGF-β, supramolecular bakuchioli, and *Terminalia chebula* extract); (A) p16; (B) p21; (C) Col-1; (D) MMP-1. Mean ± SD, n = 3.

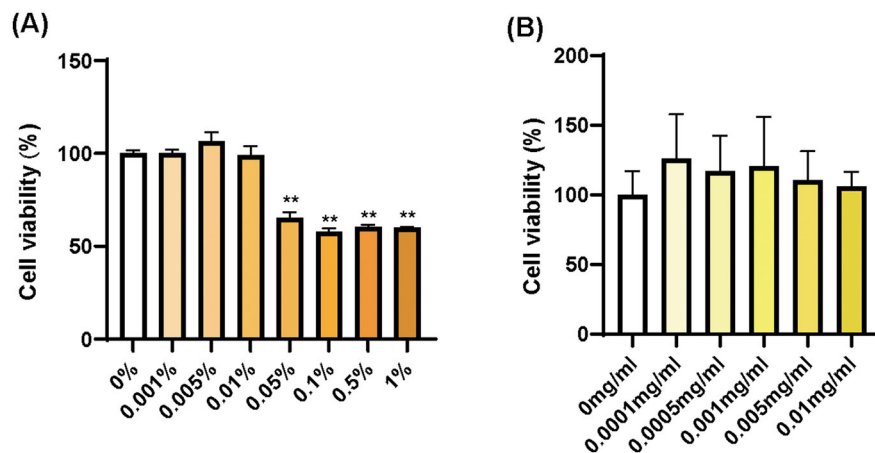


FIGURE 4 Cell viability in HSF cells for (A) supramolecular bakuchioli and (B) *Terminalia chebula* extract. Mean ± SD in (A), n = 3; in (B), n = 4.

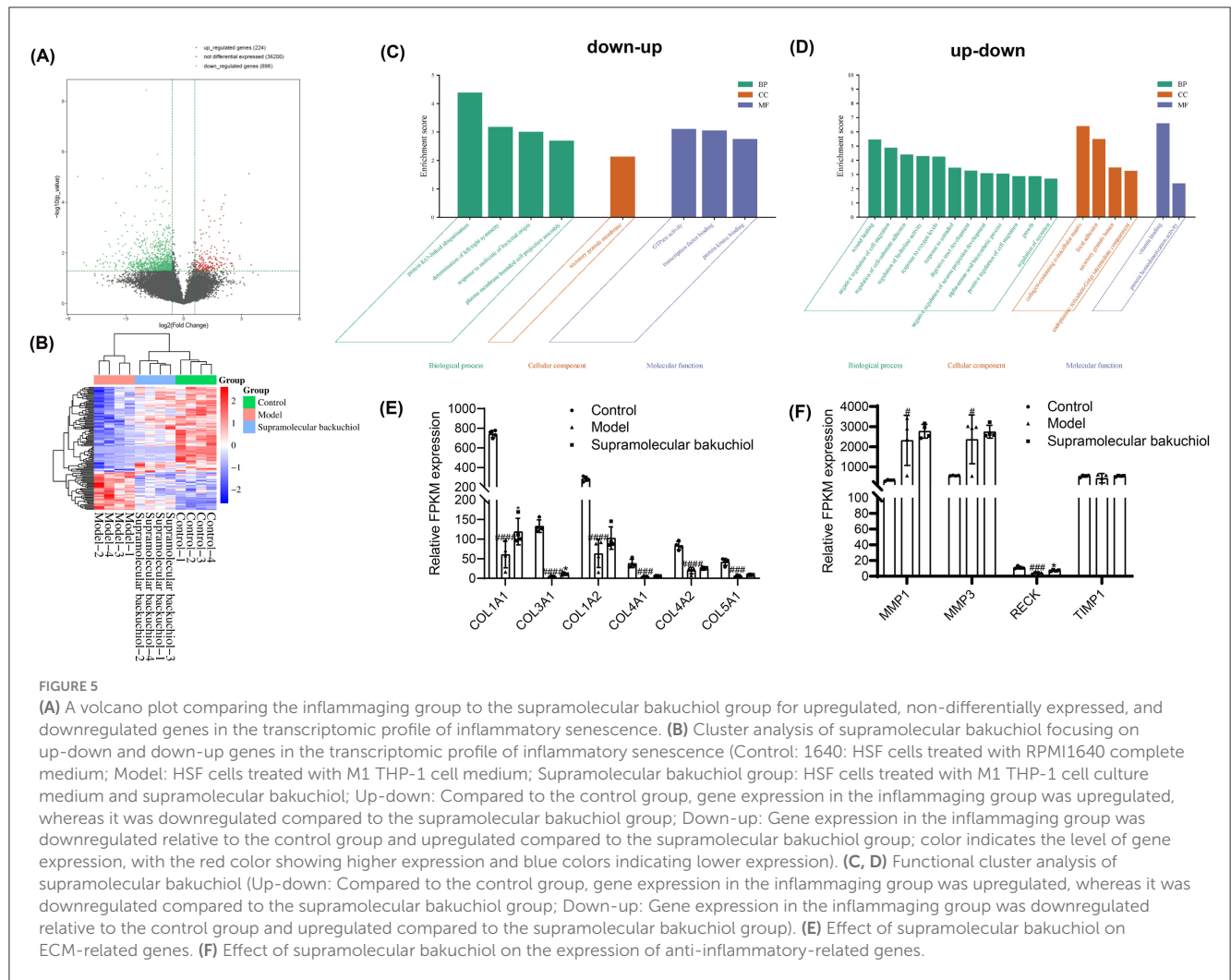
p21, and MMP-1, while upregulating the expression of Col-1 (Figure 3). This set of results confirmed the successful induction of the inflammaging process model.

3.3 Model validation by using supramolecular bakuchioli and *Terminalia chebula* extract

To validate the inflammaging models, we chose two anti-aging ingredients and identified the safe concentration range of supramolecular bakuchioli and *Terminalia chebula* extract, which

we are interested in, on HSF cells. Based on the cell viability assay, supramolecular bakuchioli shows no cytotoxicity in the concentration range of 0% to 0.01% (the concentration of bakuchioli is 0 to 0.1 mg/mL), with cell viability exceeding 90% (Figure 4A). *Terminalia chebula* extract exhibits no cytotoxicity in the concentration range of 0 to 0.01 mg/mL (Figure 4B).

Based on the cell viability test, we added supramolecular bakuchioli at a concentration of 0.001% (equivalent to 0.01 mg/mL), and *Terminalia chebula* extract at 0.003 mg/mL to the culture medium of HSF cells in our inflammaging model. Both the anti-aging ingredient supramolecular bakuchioli and the anti-inflammatory ingredient *Terminalia chebula* extract significantly downregulated the expression of p16, p21, and MMP-1



while upregulating the expression of Col-1. This indicates that both ingredients could reverse inflammaging in HSF cells, making them suitable for further application in cosmetic formulations aimed at anti-inflammatory properties (Figure 3).

3.4 RNAseq test for supramolecular bakuchiol group

To further elaborate on the difference in the inflammaging mechanism between supramolecular bakuchiol and *Terminalia chebula* extract, we extracted total RNA from the HSF cells collected in the inflammaging model. We then performed RNA sequencing and compared the RNA expression levels (FPKM value) of the different sample groups. We screened gene RNA with P values < 0.05 and $|\text{fold change}| > 1.5$. RNA with a fold change > 1.5 was labeled as upregulated genes (up), and those with a fold change < -1.5 were labeled as downregulated genes (down).

According to the volcano plot, compared to the inflammaging group, the supramolecular bakuchiol group previously upregulated 224 genes and downregulated 898 genes after

sample treatment (Figure 5A). We then focused on the upregulated and downregulated genes from the supramolecular bakuchiol group. A total of 136 significantly differentially expressed genes were identified in the control group, the inflammaging group, and the supramolecular bakuchiol group ($p < 0.05$). Compared to the control group, the inflammaging group previously upregulated 38 genes and subsequently downregulated (up-down) after sample treatment. Meanwhile, 86 genes were previously downregulated in the inflammaging group and subsequently upregulated (down-up) after sample treatment. The cluster heat map illustrates the changes in upregulated and downregulated gene expression levels in these three groups (Figure 5B).

The functions of the up-down and down-up related genes were analyzed using the GO database and were annotated with GO terms (Figures 5C, D). The results showed that up-down-related genes mainly affected the cellular molecular function of GTPase activity and the biological process of neuronal projection development. Down-up genes significantly impacted various biological processes, including wound healing, regulation of hydrolase activity, response to oxygen levels, negative regulation of cell migration, muscle structure development, extracellular matrix (ECM) biosynthesis, and alpha-amino acid biosynthesis, among others.

after sample treatment. Meanwhile, 119 genes were initially downregulated in the inflammaging group and subsequently upregulated (down-up) after sample treatment. The cluster heat map illustrates the changes in gene expression levels related to up-down and down-up statuses in these three groups (Figure 6B).

The functions of the up-down and down-up related genes were analyzed using the GO database and annotated with GO terms (Figures 6C, D). The results showed that up-down related genes were mainly enriched in the MAPK cascade and the assembly of cell processes associated with the plasma membrane in biological processes, late endosomes in cellular components, and molecular function inhibitor activity. Down-up genes have a significant impact mainly on biological processes, such as regulating classical nuclear transcription factor-kappa B (NF- κ B) signal transduction, the vascular endothelial growth factor (VEGF) signaling pathway, negative regulation of cell population proliferation, positive regulation of transmembrane transport of atoms and ions, cellular response to lipids, and regulation of cell cycle progression, among others.

MAPK cascades have been implicated in various cellular processes, including proliferation, differentiation, apoptosis, cell survival, motility, metabolism, stress response, and inflammation. MAP4K2 acts as a MAP kinase kinase kinase (MAP4K), serving as an upstream activator of the stress-activated protein kinase/c-Jun N-terminal kinase (SAP/JNK) signaling pathway and also activating the p38 MAPKs signaling pathway. According to the sequencing results, *MAP4K2* gene expression is significantly upregulated in senescent HSF cells (Figure 6E). The expression of *MAP4K2* can be inhibited following treatment with *Terminalia chebula* extract. CCL3 is a factor with both inflammatory and chemotactic properties. As shown in Figure 5C, CCL3 was significantly reduced after treatment with *Terminalia chebula* extract, indicating that *Terminalia chebula* extract can inhibit inflammaging by reducing cell senescence and the accumulation of inflammatory factors.

4 Discussion

Sensitive skin tends to react to oxidative stress and other stimulating factors that can lead to skin inflammation and result in inflammaging, which is a new branch of aging-related research (3, 31). Effective *in vitro* models for sensitive skin are needed to screen anti-inflammaging cosmetic ingredients rapidly, rather than traditional animal models or clinical studies that have been used thus far (14, 15). However, there is a lack of an ingredient screening method specifically designed for inflammaging. To further improve research methods on sensitive skin and determine the anti-inflammaging properties, we established an *in vitro* inflammaging model. In this model, THP-1 cells were induced into an M1 phenotype with upregulated expression of inflammatory factors such as CD86, TNF- α , IL-1 β , and IL-6. Next, the supernatant from the M1 THP-1 cell culture was applied to induce aging in HSF cells. Cellular

senescence and skin aging indicators p16, p21, and MMP-1 were upregulated, while Col-1 was downregulated, indicating that the *in vitro* cellular model system of inflammaging was successfully constructed.

Additionally, two ingredients, supramolecular bakuchiol and *Terminalia chebula* extract, were utilized to evaluate the feasibility of this system and validate their efficacy against inflammaging. Both supramolecular bakuchiol and *Terminalia chebula* extract were confirmed to reverse inflammaging in this model by downregulating p16, p21, and MMP-1 while upregulating the production of Col-1. Supramolecular bakuchiol comprises the anti-aging component bakuchiol combined with the anti-inflammatory ingredient matrine, which enhances collagen production and inhibits cellular inflammation. Conversely, *Terminalia chebula* extract is reported to have anti-inflammatory properties, allowing it to neutralize inflammatory factors in the M1 supernatant and reduce inflammation in HSF cells.

Moreover, transcriptomics was used to investigate the mechanisms of supramolecular bakuchiol and *Terminalia chebula* extract concerning the reversal of inflammaging. In our study, we found these two ingredients have distinct regulatory mechanisms on inflammaging. Supramolecular bakuchiol enhances collagen production by promoting the gene transcription of *COL1A1* and *COL3A3*, while it inhibits inflammatory factors by increasing the transcription of anti-inflammatory genes [*PTX3* (26, 27), *ADAM33* (28, 29), and *PDLIM1* (30)]. Conversely, *Terminalia chebula* extract can inhibit cell senescence by directly reducing the transcription of *MAP4K2* (32) or by decreasing the accumulation of inflammatory factors, such as CCL3 (33). Our study aligns with previous research indicating that supramolecular bakuchiol primarily exhibits anti-aging properties, while *Terminalia chebula* extract is primarily anti-inflammatory.

Based on this study, we developed a novel *in vitro* model of skin inflammaging using M1 macrophage supernatant to induce HSF cell aging and examined the anti-inflammaging mechanism of *Terminalia chebula* extract and supramolecular bakuchiol with this model. In the future, we aim to enhance the experimental system and broaden the application scope of the inflammaging model to detect not only the direct inflammaging mechanism, primarily between fibroblasts and immune cells but also the indirect inflammaging mechanism, involving keratinocytes that produce ROS to induce aging. Additionally, considering the differences between cell lines and *in vivo* tissues, we will further explore the inflammaging model on a 3D skin model that more closely resembles native tissue and investigate the effects of keratinocytes, fibroblasts, and other common skin cells.

Data availability statement

The data discussed in this publication have been deposited in NCBI's Gene Expression Omnibus (Edgar et al., 2002) and are accessible through GEO Series accession number GSE286316 (<https://www.ncbi.nlm.nih.gov/geo/query/acc.cgi?acc=GSE286316>).

Ethics statement

Ethical approval was not required for the studies on humans in accordance with the local legislation and institutional requirements because only commercially available established cell lines were used.

Author contributions

YX: Formal analysis, Investigation, Methodology, Supervision, Validation, Writing – original draft, Writing – review & editing. YLiu: Project administration, Writing – original draft. JL: Methodology, Writing – review & editing. YLi: Data curation, Formal analysis, Investigation, Validation, Writing – review & editing. LX: Investigation, Writing – review & editing. KD: Investigation, Writing – review & editing. XL: Methodology, Supervision, Writing – review & editing. TZ: Methodology, Supervision, Writing – review & editing.

Funding

The author(s) declare financial support was received for the research and/or publication of this article. This work was funded

References

- Dorf N, Maciejczyk M. Skin senescence—from basic research to clinical practice. *Front Med.* (2024) 11:1484345. doi: 10.3389/fmed.2024.1484345
- O'Reilly S, Markiewicz E, Idowu OC. Aging, senescence, and cutaneous wound healing—a complex relationship. *Front Immunol.* (2024) 15:1429716. doi: 10.3389/fimmu.2024.1429716
- Zhang J, Yu H, Man MQ, Hu L. Aging in the dermis: fibroblast senescence and its significance. *Aging Cell.* (2024) 23:e14054. doi: 10.1111/acel.14054
- López-Otín C, Blasco MA, Partridge L, Serrano M, Kroemer G. Hallmarks of aging: an expanding universe. *Cell.* (2023) 186:243–78. doi: 10.1016/j.cell.2022.11.001
- Coperchini F, Greco A, Teliti M, Croce L, Chytiris S, Magri F, et al. Inflammageing: how cytokines and nutrition shape the trajectory of ageing. *Cytokine Growth Factor Rev.* (2024) 8:4. doi: 10.1016/j.cytogfr.2024.08.004
- Ferreira MS, Sousa Lobo JM, Almeida IF. Sensitive skin: active ingredients on the spotlight. *Int J Cosmet Sci.* (2022) 44:56–73. doi: 10.1111/ics.12754
- Ho CY, Dreesen O. Faces of cellular senescence in skin aging. *Mech Ageing Dev.* (2021) 198:111525. doi: 10.1016/j.mad.2021.111525
- Augello FR, Lombardi F, Ciafarone A, Ciummo V, Altamura S, Giuliani M, et al. Efficacy of an innovative poly-component formulation in counteracting human dermal fibroblast aging by influencing oxidative and inflammatory pathways. *Biomedicine.* (2024) 12:2410. doi: 10.3390/biomedicine12092030
- Zagórska-Dziok M, Mokrzyńska A, Ziemlewska A, Nizioł-Lukaszewska Z, Sowa I, Feldo M, et al. Assessment of the antioxidant and photoprotective properties of *Cornus mas* L. extracts on HDF, HaCaT and A375 cells exposed to UVA radiation. *Int J Mol Sci.* (2024) 25:10993. doi: 10.3390/ijms252010993
- Peng X, Liu N, Zeng B, Bai Y, Xu Y, Chen Y, et al. High salt diet accelerates skin aging in wistar rats: an 8-week investigation of cell cycle inhibitors, SASP markers, oxidative stress. *Front Bioeng Biotechnol.* (2024) 12:1450626. doi: 10.3389/fbioe.2024.1450626
- Stalder JF, Tennstedt D, Deleuran M, Fabbrocini G, de Lucas R, Haftek M, et al. Fragility of epidermis and its consequence in dermatology. *J Eur Acad Dermatol Venereol.* (2014) 28:1–18. doi: 10.1111/jdv.12509
- Aslam A, Bahadar A, Liaquat R, Saleem M, Waqas A, Zwawi M. Algae as an attractive source for cosmetics to counter environmental stress. *Sci Total Environ.* (2021) 772:144905. doi: 10.1016/j.scitotenv.2020.144905

by the Natural Science Basic Research Plan in Shaanxi Province of China (2024JC-YBMS-605).

Conflict of interest

YX, YLiu, and TZ were employed by Better Way (Shanghai) Cosmetics Co. Ltd.

The remaining authors declare that the research was conducted in the absence of any commercial or financial relationships that could be construed as a potential conflict of interest.

Generative AI statement

The author(s) declare that no Gen AI was used in the creation of this manuscript.

Publisher's note

All claims expressed in this article are solely those of the authors and do not necessarily represent those of their affiliated organizations, or those of the publisher, the editors and the reviewers. Any product that may be evaluated in this article, or claim that may be made by its manufacturer, is not guaranteed or endorsed by the publisher.

- Zhang Y, Li T, Zhao H, Xiao X, Hu X, Wang B, et al. High-sensitive sensory neurons exacerbate rosacea-like dermatitis in mice by activating $\gamma\delta$ T cells directly. *Nat Commun.* (2024) 15:7265. doi: 10.1038/s41467-024-50970-1
- Huang B, Wang X, Bu L, Zhang Y, Liu X, Liang F, et al. Construction of a mouse model for sensitive skin research. *Contact Dermatitis.* (2024) 91:327–41. doi: 10.1111/cod.14652
- Zhang J, Liu S, Guo W, Li N, Huang Y. A highly efficient and user-friendly sensitive skin model on the forearm. *J Cosmet Dermatol.* (2024) 24:e16619. doi: 10.1111/jocd.16619
- Spierings NMK. Cosmetic commentary: is bakuchiol the new “skincare hero”? *J Cosmet Dermatol.* (2020) 19:3208–9. doi: 10.1111/jocd.13708
- Cariola A, Chami ME, Granatieri J, Valgimigli L. Anti-tyrosinase and antioxidant activity of meroterpenoid bakuchiol from *Psoralea corylifolia* (L.). *Food Chem.* (2023) 405:134953. doi: 10.1016/j.foodchem.2022.134953
- Chaudhuri RK, and Bojanowski K. Bakuchiol: a retinol-like functional compound revealed by gene expression profiling and clinically proven to have anti-aging effects. *Int J Cosmet Sci.* (2014) 36:221–30. doi: 10.1111/ics.12117
- Wang M, Wang Z, Zhang J, Zhang L, Wang W, Zhan J, et al. A matrine-based supramolecular ionic salt that enhances the water solubility, transdermal delivery, and bioactivity of salicylic acid. *Chem Eng J.* (2023) 468:143480. doi: 10.1016/j.cej.2023.143480
- Ekambaram SP, Aruldas J, Srinivasan A, Erusappan T. Modulation of NF- κ B and MAPK signalling pathways by hydrolysable tannin fraction from *Terminalia chebula* fruits contributes to its anti-inflammatory action in RAW 2647 cells. *J Pharm Pharmacol.* (2022) 74:718–29. doi: 10.1093/jpp/rgab178
- Horiba S, Kami R, Tsutsui T, Hosoi J. IL-34 downregulation-associated M1/M2 macrophage imbalance is related to inflammaging in sun-exposed human skin. *JID Innov.* (2022) 2:100112. doi: 10.1016/j.xjidi.2022.100112
- Lu B, Wang Z, Xu Y, Liu Y, Ruan B, Zhang J, et al. Anti-aging and anti-inflammatory fulfilled through the delivery of supramolecular bakuchiol in ionic liquid. *Supramolec Mater.* (2025) 4:100093. doi: 10.1016/j.supmat.2025.100093
- Zhang Y, Yang L, Dai G, Cao H. Knockdown of PHGDH potentiates 5-FU cytotoxicity in gastric cancer cells via the Bcl-2/Bax/caspase-3 signaling pathway. *Int J Clin Exp Pathol.* (2018) 11:5869–76.

24. Tang D, Chen M, Huang X, Zhang G, Zeng L, Zhang G, et al. SRplot: a free online platform for data visualization and graphing. *PLoS ONE*. (2023) 18:e0294236. doi: 10.1371/journal.pone.0294236
25. Faria AVS, Andrade SS. Decoding the impact of ageing and environment stressors on skin cell communication. *Biogerontology*. (2024) 26:3. doi: 10.1007/s10522-024-10145-3
26. Salvato M, Frizzera F, Ghirardello A, Calligaro A, Botsios C, Zen M, et al. Anti-pentraxin 3 antibodies and residual disease activity in rheumatoid arthritis. *Rheumatology*. (2024) 28:keae529. doi: 10.1093/rheumatology/keae529
27. Madkour S, Mostafa MG, El-Kady H. The assessment of pentraxin 3: a diagnostic and prognostic biomarker in lower respiratory tract infections in children. *Ital J Pediatr*. (2024) 50:182. doi: 10.1186/s13052-024-01735-5
28. Yan F, Hu X, He L, Jiao K, Hao Y, Wang J. ADAM33 silencing inhibits vascular smooth muscle cell migration and regulates cytokine secretion in airway vascular remodeling via the PI3K/AKT/mTOR pathway. *Can Respir J*. (2022) 2022:8437348. doi: 10.1155/2022/8437348
29. Johnathan M, Muhamad SA, Gan SH, Stanslas J, Fuad WEM, Hussain FA, et al. *Lignosus rhinocerotis* Cooke Ryvariden ameliorates airway inflammation, mucus hypersecretion and airway hyperresponsiveness in a murine model of asthma. *PLoS ONE*. (2021) 16:e0249091. doi: 10.1371/journal.pone.0249091
30. Yang L, Yuan L, Liu G. Comprehensive evaluation of disulfidptosis in intestinal immunity and biologic therapy response in Ulcerative Colitis. *Heliyon*. (2024) 10:e34516. doi: 10.1016/j.heliyon.2024.e34516
31. Xia S, Zhang X, Zheng S, Khanabdali R, Kalionis B, Wu J, et al. An update on inflammaging: mechanisms, prevention, and treatment. *J Immunol Res*. (2016) 2016:8426874. doi: 10.1155/2016/8426874
32. Schreiber A. A non-canonical role: the Hippo pathway regulator MAP4K2 controls autophagy and cell survival upon energy stress. *Mol Cell*. (2023) 83:3043–5. doi: 10.1016/j.molcel.2023.08.020
33. Yang Z, Liu M, Chang Z, Du C, Yang Y, Zhang C, et al. Myeloid-derived growth factor promotes M2 macrophage polarization and attenuates Sjögren's syndrome via suppression of the CX3CL1/CX3CR1 axis. *Front Immunol*. (2024) 15:1465938. doi: 10.3389/fimmu.2024.1465938